Electronic Supplementary Material (ESI) for Environmental Science: Water Research & Technology.
This journal is © The Royal Society of Chemistry 2020

Application of liquid-infused membranes to mitigate biofouling

Hanieh Bazyar,[a,b] Linya Xu,[b] Hendrik Jan de Vries,[b] Slawomir Porada,[a,b] and Rob G. H. Lammertink,[*a]

[a] Department of Science and Technology, Soft Matter, Fluidics and Interfaces (SFI), University of Twente, Enschede, The Netherlands.

[b] Wetsus, European centre of excellence for sustainable water technology, Leeuwarden, The Netherlands.

[*] Correspondence to: r.g.h.lammertink@utwente.nl

Supporting Information (SI)

Membrane characterization

The commercial PVDF membrane (HVHP00010) is characterized using scanning electron microscopy (SEM) (JEOL 5600 LV) and capillary flow porometer (Porolux-1000). The SEM images of top, bottom and cross section of the membrane are shown in Figure S1.

Capillary flow porometry measurement on the commercial PVDF membrane is done by pushing nitrogen gas through the membrane infused with a low surface tension liquid, i.e. Fluorinert FC-43, at different pressure values. The corresponding gas flow rate is measured simultaneously. Figure S2(a) shows the nitrogen gas flow rate as a function of pressure for the PVDF membrane. This measurement is conducted in two runs: in the first run, the so called wet curve, a sudden increase in gas flow rate is observed which corresponds to the pressure where the biggest pores are opened (first bubble point (FBP)). In the second run as the liquid has been already pushed out, a linear behaviour between flow and pressure is obtained (dry curve). The point where wet and dry curves meet corresponds to the smallest pore size. The half-dry curve is also plotted where the flow values are half of the flow values of the dry curve. The crossing point of this curve and wet curve determines the mean flow pore size (MFP). The Young-Laplace equation

$$\Delta P = \frac{2\gamma|\cos\theta_E|}{r}, \tag{S1}$$

by considering total wetting (θ_E=180°) is used to relate pressure to the pore size. In Equation (S1), r is the pore radius (m), γ is the interfacial tension (N/m) between permeating fluid and liquid, and θ_E is the advancing contact angle (larger than 90°) of the permeating fluid with respect to the pore wall.

Based on the results of this measurement, the pore size distribution of the membrane can be obtained which is shown in Figure S2(b). As can be seen in Figure S2, the commercial PVDF membrane has a narrow pore size distribution with an average pore radius of 0.51 μm and size distribution of 0.043 μm (full width at half max/2).

The contact angle measurement on dry and liquid-infused membrane (K101-infused) is performed using contact angle Goniometer (Dataphysics OCA20). Static contact angle measurement is performed by dispensing a 2 μl water drop on the membrane surface. At least 6 independent static measurements are performed on different spots of the membrane surface. Dynamic measurements (advancing-receding contact angle (ARCA)) are performed within six cycles by placing the needle in the 2μl-drop (sessile drop needle-in mode) and continuously supplying or withdrawing water up to 6 μl at the rate of 0.5 μl/min. The delay time between each cycle (advancing and receding measurement) is 2 s. The average results of all the measurements results are shown in Table S1. A lower contact angle hysteresis and subsequently higher droplet mobility are observed for liquid-infused membrane compared to dry membrane. However, contact angle hysteresis of liquid-infused membrane is not $< 5°$ which implies "slipperiness"[1]. This is possibly due to the presence of hydrophilic impurities in the PVDF membrane reported by the manufacturer.

Liquid-liquid displacement (LLD) analysis

In order to better understand the retention of the infusion liquid in the liquid-infused membrane after water is pushed through the membrane, liquid-liquid displacement (LLD) experiment is done. The schematic of the set-up is shown in Figure S3(a). A Bronkhorst mass flow controller (mini CORI-FLOW M14) and pressure meter (IN-PRESS P-502CI) which are connected using a control valve (COMBI-FLOW Mass flow C5I) are used. The LLD experiment is performed in four different cycles. Each cycle is carried out in a flux-increasing mode, which is done twice starting from zero up to a certain flux value. In each run, the flux is increased step-wise. At each step, flux is kept constant for 100 s and the pressure is reported for the last 40 s of each step[1]. The result is shown in Figure S3(b).

In order to check for the presence of the infusion liquid in the membrane after the experiment, the obtained results are compared with the results of the pre-wet membrane (see Figure S3). To make the pre-wet membrane first the membrane was infused with 15.5 μl cm^{-2} ethanol. Then the ethanol-infused membrane was kept in a beaker with 200 ml of MQ water overnight. This is done to make sure that the ethanol in the membrane pores are replaced with water. The permeability of pre-wet as well as liquid-infused membranes is calculated using Darcy's law[2]

$$Q = \frac{\kappa a}{\mu}\frac{dp}{dx}. \tag{S2}$$

Here and in the following, Q is the volumetric flow of the permeating fluid (in this case water) (m^3/s), κ is the permeability (m^2), a is the total area of the membrane (m^2), μ is the viscosity

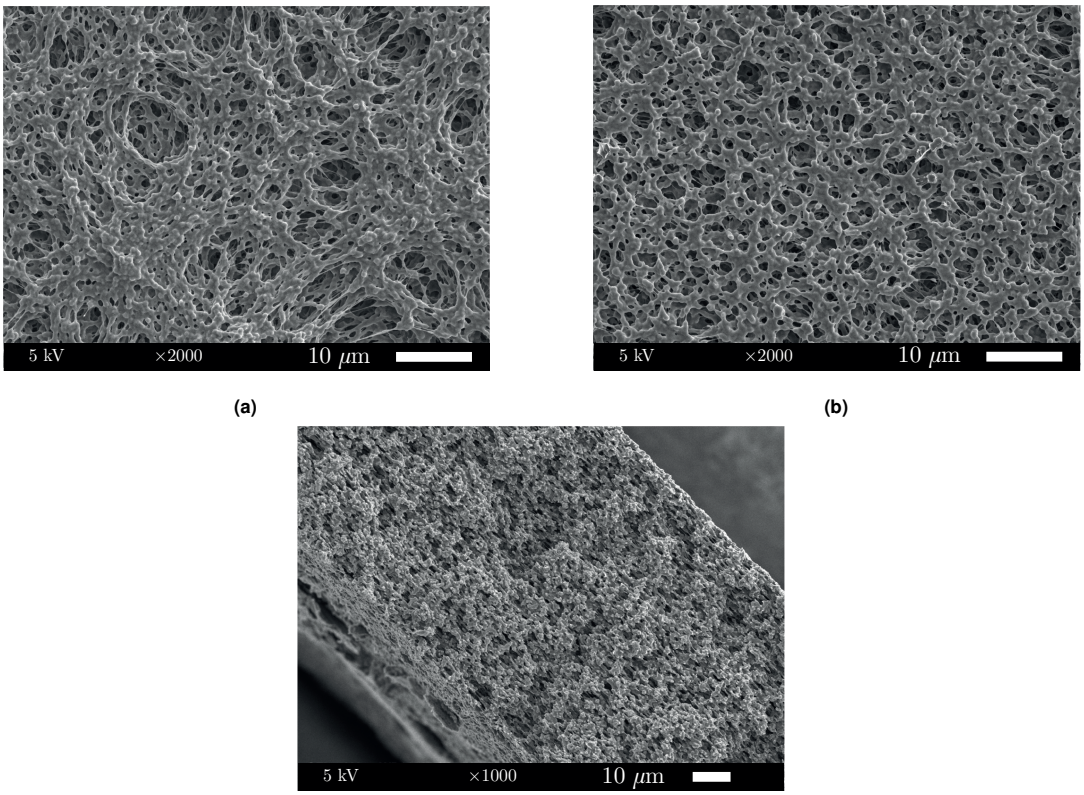

Fig. S1 Scanning electron microscopy (SEM) images of the commercial PVDF membrane from Merck (HVHP00010). **(a)** Top surface, **(b)** bottom surface, **(c)** cross section.

Table S1 Static and ARCA measurements on dry and K101-infused commercial PVDF membranes (values after $\pm$ are the corresponding standard deviation).

Sample	Contact angle (°)			
	Mean Static	Advancing (θ_{Adv})	Receding (θ_{Rec})	Hysteresis
Dry membrane	121.90$\pm$0.49	124.38$\pm$0.53	97.86$\pm$2.99	26.53$\pm$2.64
K101-infused	104.24$\pm$1.18	106.12$\pm$1.35	87.54$\pm$1.71	18.58$\pm$1.38

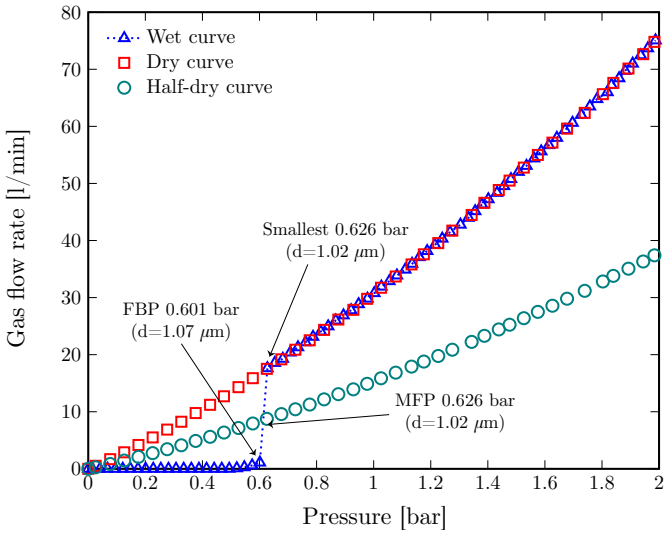

(a)

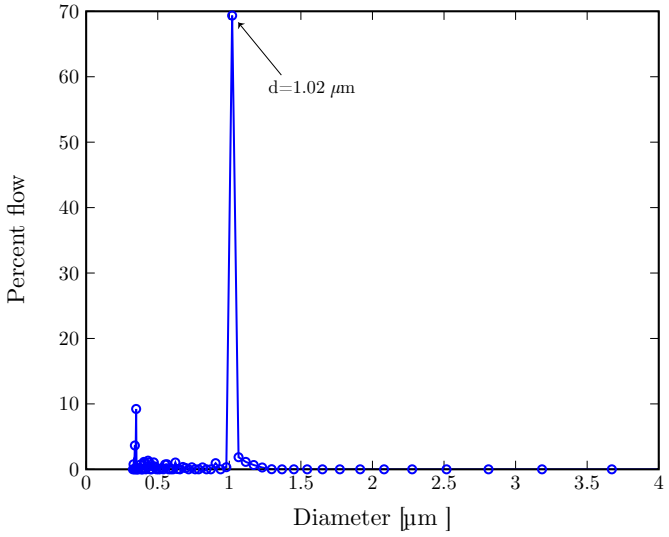

(b)

Fig. S2 Capillary flow porometry results of the commercial PVDF membrane. **(a)** Flow rate of nitrogen gas as a function of pressure. The corresponding pressure values for the biggest pore size (first bubble point (FBP)), mean flow pore size (MFP), and smallest pore size are indicated with arows. **(b)** Pore size distribution of the membrane.

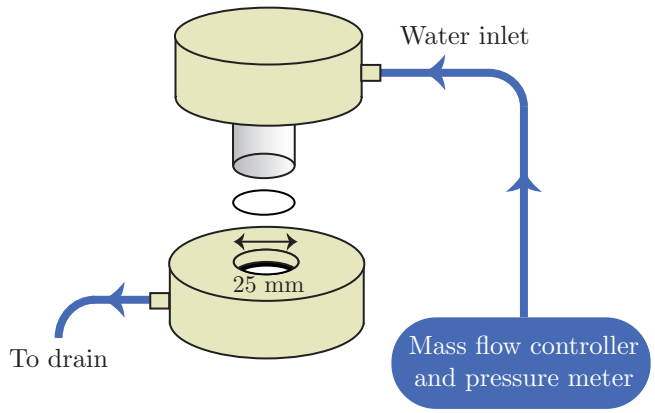

(a)

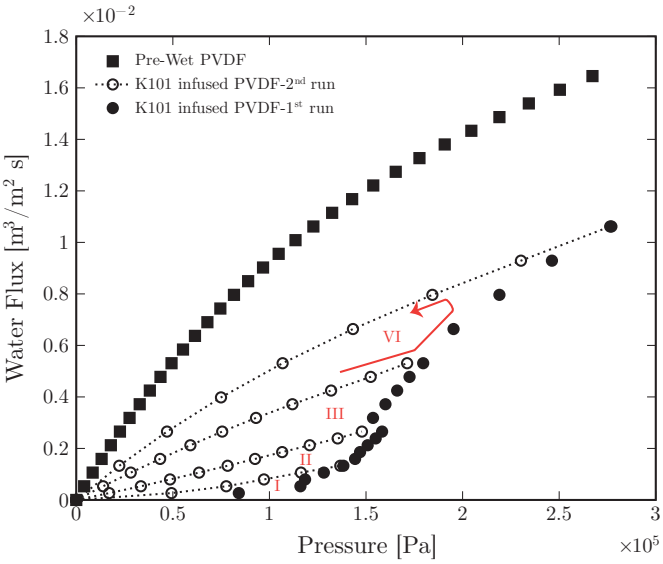

(b)

Fig. S3 (a) The set-up used for liquid-liquid displacement (LLD) experiment. **(b)** Successive LLD experiment in a flux controlled mode on Krytox 101-infused PVDF membrane using hexadecane. LLD is done in four different cycles (I-IV) and each cycle consists of a 1st (filled symbols) and a 2nd run (open symbols). In each run flux is increased step-wise from zero up to a certain maximum value and pressure is measured correspondingly. A typical sequence of the measurement is shown for cycle IV.

Table S2 Comparison of permeability and fraction of active pores for three different cycles of liquid-infused membrane and for the dry case.

Membrane	Permeability (κ) (Darcy*)	Estimated fraction of active pores
LIM-cycle 1	7.99×10^{-4}	0.16
LIM-cycle 2	1.46×10^{-3}	0.29
LIM-cycle 3	2.49×10^{-3}	0.49
LIM-cycle 4	3.06×10^{-3}	0.61
Pre-wet	5.03×10^{-3}	1

*1 Darcy $=0.987\times10^{-12}$ m^2

of the displacing fluid (Pa s), $\frac{dp}{dx}$ is the pressure gradient across the membrane thickness (Pa/m), r is the mean pore radius (m), and ϕ is porosity. A simple model is then used to relate permeability to porosity ϕ, namely [1]

$$\kappa = \frac{\phi r^2}{24}. \tag{S3}$$

The calculated porosity is a measure of opened and active pores for water transport in the membrane. The results of the calculated permeability and the estimated fraction of the active pores are shown in Table S2 (membrane thickness and water viscosity are considered as 80 μm and 1 mPa s respectively). This fraction is the ratio between the calculated porosity for the liquid-infused membrane in each cycle and that of the pre-wet membrane. The permeability of the liquid-infused membrane increases in each cycle, revealing that new pores are opened for water transport. The lower permeability values of liquid-infused membrane (LIM) in comparison with pre-wet membrane suggests incomplete removal of the infusion liquid with around 39% retained infusion liquid in the membrane. For more information on this kind of analysis, we refer the reader to our other work [1].

Pictures of feed and permeate spacers

Figures S4(a) and S4(b) show the pictures of the feed and permeate spacers respectively.

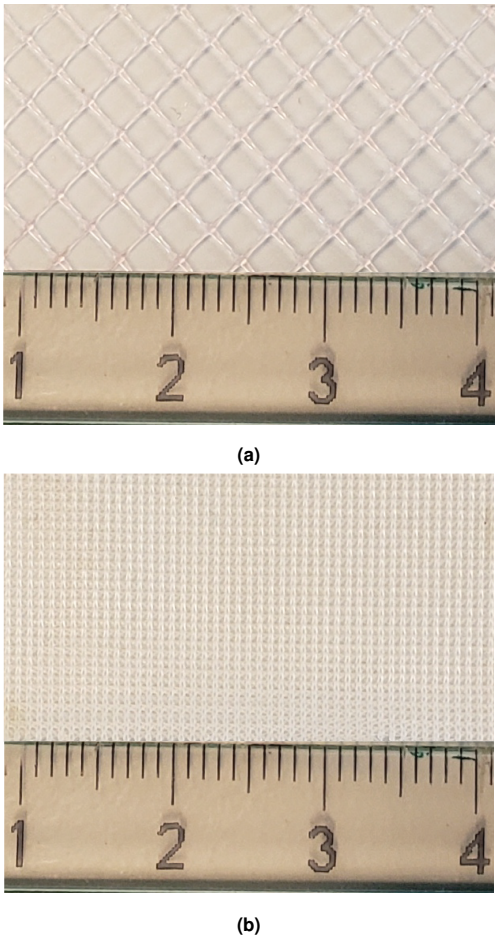

Fig. S4 Pictures of **(a)** feed spacer and **(b)** permeate spacer used in the cross flow filtration module.

Results of feed pressure increase

The feed pressure increase during the bio-fouling experiment was also monitored. The results for both dry and liquid-infused membranes with the presence of the feed spacer in the membrane module is shown in Figure S5. Lower feed pressure increase at a certain time is observable for liquid-infused membrane compared to dry membrane. This further shows that less bacteria is formed on the surface of the liquid-infused membrane compared to that of the dry membrane due to the presence of the infusion liquid.

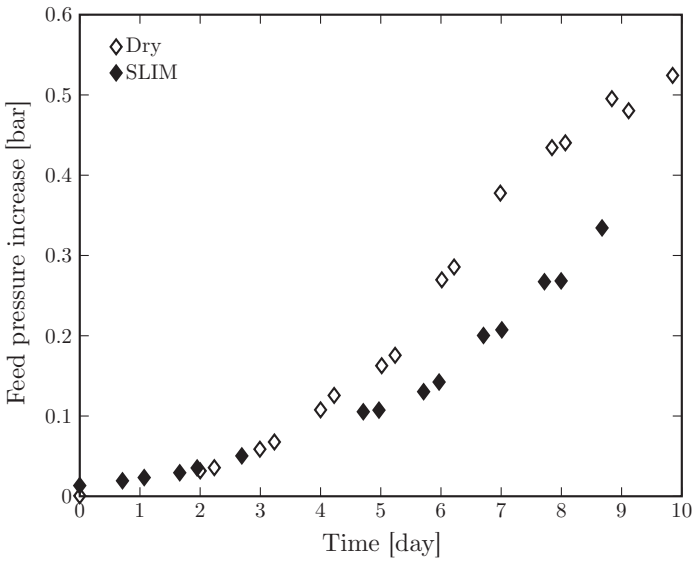

Fig. S5 Feed pressure increase as a function of time during biofouling experiments for both dry and liquid-infused membranes with presence of the feed spacer in the cell configuration.

Effect of nutrient concentration

The effect of nutrient concentration on bacterial growth is investigated by increasing the nutrient concentration to 7.2 g CH_3COONa, 1.1 g $NaH_2PO_4.2H_2O$, and 2.6 g $NaNo_3$. The results of TMP and feed pressure increase are shown in Figure S6. The lower increase in both TMP and feed pressure for liquid-infused membrane compared to dry membrane confirm improved perfor-

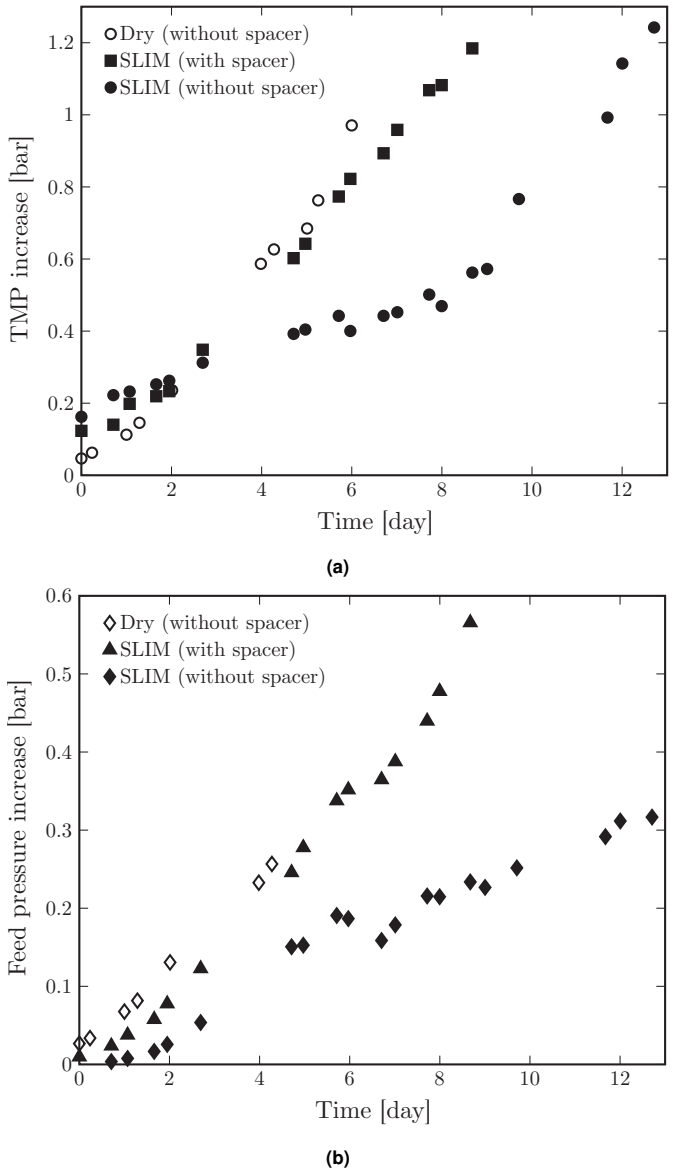

Fig. S6 (a) TMP increase and **(b)** feed pressure increase for both dry and liquid-infused membranes in biofouling experiments performed with higher concentration of nutrients.

mance of liquid-infused membranes in mitigation of bio-fouling. The increase in both TMP and feed pressure of liquid-infused membrane in the presence of the feed spacer in the membrane monitor can be attributed to the effect of spacer in acceleration of bacterial formation and growth. This is explained more in the main paper.

Confocal laser scanning microscope (CLSM) images

Figure S7 shows images obtained from z-stack of CLSM at different depths. Figures S7(a) and S7(b) demonstrate closest plane to the biofilm surface (feed water solution side). The closest plane to the membrane area is shown in Figures S7(c) and S7(d).

Modification of logistic model

The fitting parameters (a, b, and c) for both membranes with different cell configurations are shown in Table S3. Based on definition of biological parameters (see main paper, section "Modeling of bacterial growth curve"), one can determine the modified logistic model accordingly.

The sigmoidal logistic model (Equation 1 in the main paper) can be rewritten as

$$y = a.[1 + exp(b - ct)]^{-1}. \tag{S4}$$

The first and second derivatives of Equation S4 are respectively

$$\frac{dy}{dt} = ac\ exp(b - ct).[1 + exp(b - ct)]^{-2} \tag{S5}$$

and

$$\frac{d^2y}{dt^2} = ac^2 exp(b - ct).[1 + exp(b - ct)]^{-3}.[exp(b - ct) - 1]. \tag{S6}$$

The inflection point is where the second derivative is zero, i.e. $exp(b - ct) - 1 = 0$. Therefore $t_{\mathrm{i}} = \frac{b}{c}$ and the corresponding y value at the inflection point using Equation S4 is equal to $\frac{a}{2}$. The specific growth rate (μ_{m}) is then the first derivative (Equation S5) at the inflection point, i.e.

$$\frac{dy}{dt}|_{t=t_{\mathrm{i}}} = \mu_{\mathrm{m}} = \frac{ac}{4}. \tag{S7}$$

By knowing one point ($\frac{b}{c}$, $\frac{a}{2}$) and the slope of the tangent line ($\frac{ac}{4}$), one can describe the tangent line as

$$y = \frac{ac}{4}t - \frac{a(b-2)}{4}. \tag{S8}$$

Lag period λ is defined as the t-axis intercept of the tangent line (Equation S8 = 0). Therefore λ is calculated as

$$\lambda = \frac{b-2}{c}. \tag{S9}$$

Asymptotic value A is reached when t$\rightarrow \infty$ in Equation S4. By considering that,

$$t \rightarrow \infty \Rightarrow y = a \Rightarrow A = a. \tag{S10}$$

The mathematical parameters a, b, and c can be calculated based on biological parameters, λ, μ_{m}, and A using Equations S10, S9, and S7 respectively. By substituting these mathematical parameters in logistic model (Equation S4) one can define the modified logistic model (Equation 2 in the main paper).

Linear regression

The R^2 values of the linear fit to the exponential phase together with the root mean square error (RMSE) and summation of square error (SSE) are shown in Table S4 for different cell configurations. As it is evident a relatively good fit was obtained for all the results. The obtained duration of the lag phase, i.e. λ directly from the graph of $\ln(\frac{P}{P_0})$ as a function of time for different cell configurations is shown in Table S5.

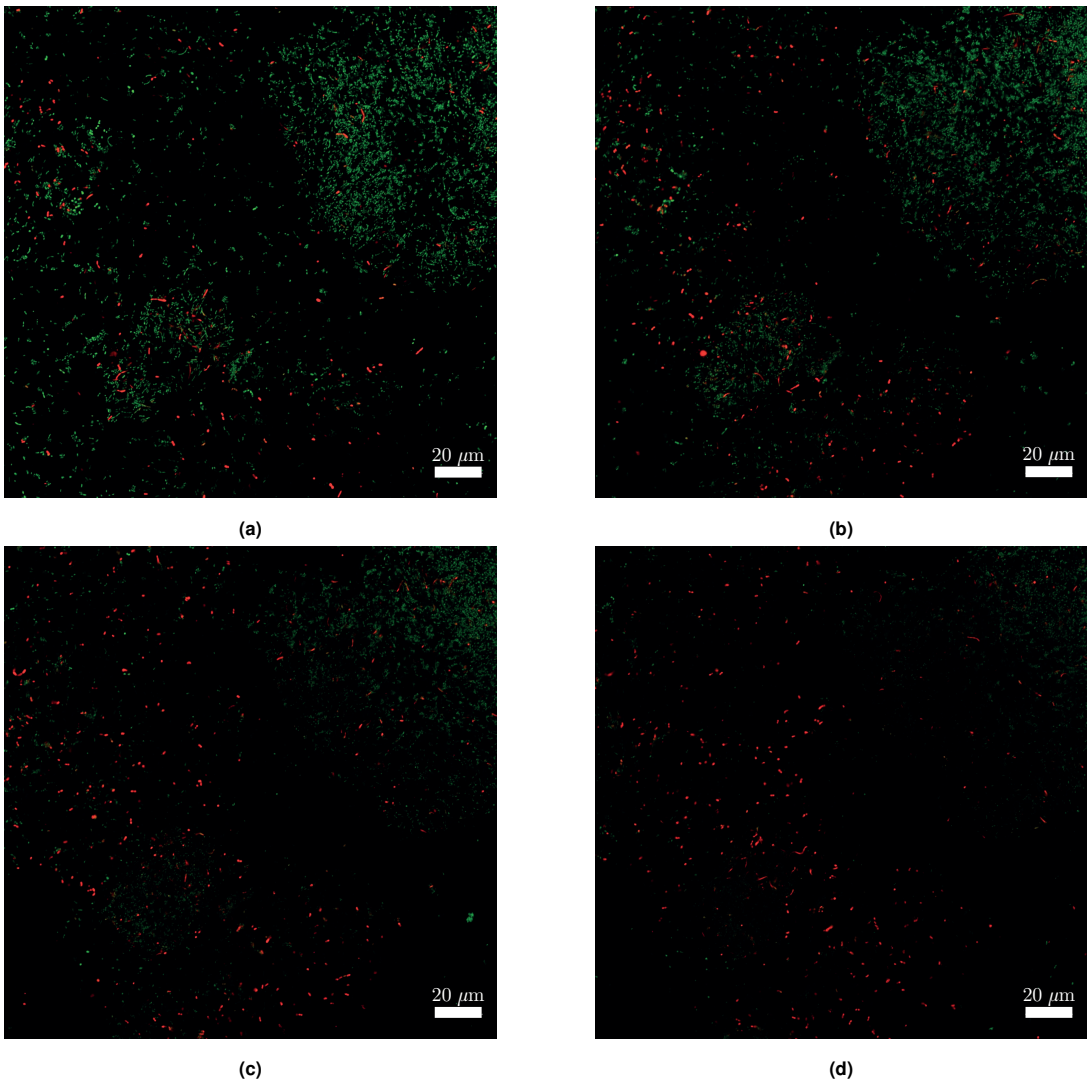

Fig. S7 CLSM images of the biofilm (green and red respectively show live and dead cells) from the surface of LIM-without spacer at different depths of **(a)** 1.33 μm (side facing the feed water channel), **(b)** 3.56 μm, **(c)** 5.78 μm, and **(d)** 8.01 μm (side facing the membrane surface).

Table S3 Fitting parameters of fitted experimental data points of $\ln(\frac{P}{P_0})$ as a function of time to logistic model (Equation S4) (all the values after $\pm$ are half of the the 95% confidence interval limits ((Upper CI - Lower CI)/2)).

Membrane and cell configuration	Fitting parameters		
	a (-)	b (-)	c (-)
Dry-without spacer	4.41$\pm$0.12	2.82$\pm$0.16	0.31$\pm$0.02
Dry-with spacer	3.64$\pm$0.13	3.56$\pm$0.34	0.72$\pm$0.08
LIM-without spacer	0.48$\pm$0.04	6.48$\pm$0.91	0.44$\pm$0.07
LIM-with spacer	0.64$\pm$0.04	2.46$\pm$0.17	0.43$\pm$0.05

Table S4 Accuracy of the linear regression of the experimental data points of $\ln(\frac{P}{P_0})$ as a function of time.

Membrane and cell configuration	Goodness of linear fit to exponential phase		
	R^2	RMSE	SSE
Dry-without spacer	0.979	0.156	0.438
Dry-with spacer	0.986	0.102	0.073
LIM-without spacer	0.988	0.013	0.001
LIM-with spacer	0.969	0.021	0.004

Table S5 The values of the lag phase λ obtained directly from the graph of $\ln(\frac{P}{P_0})$ as a function of time.

Membrane and cell configuration	λ
Dry-without spacer	2.001
Dry-with spacer	2.235
LIM-without spacer	9.004
LIM-with spacer	0.000

References

1 H. Bazyar, P. Lv, J. A. Wood, S. Porada, D. Lohse and R. G. H. Lammertink, Liquid-liquid displacement in slippery liquid-infused membranes (SLIMs), *Soft Matter*, 2018, **14**, 1780–1788.

2 H. Darcy, *Les Fontaines Publiques de la Ville de Dijon*, Victor Dalmont, Paris, Paris, 1856.